Fermi National Accelerator Laboratory

FERMILAB-Conf-91/81-A
March 1991

A PROPOSED SEARCH FOR DARK-MATTER AXIONS IN THE 0.6-16 μeV RANGE

Karl van Bibber
Lawrence Livermore National Laboratory
P.O. Box 808, Livermore, CA 94550

P. Sikivie, N.S. Sullivan, D.B. Tanner
Department of Physics, University of Florida
Gainesville, FL 32611

M.S. Turner
Department of Physics and Astronomy, University of Chicago
Chicago, IL 60637-1433

and

NASA/Fermilab Astrophysics Center, Fermi National Accelerator
Laboratory, Batavia, IL 60510-0500

D.M. Moltz
Nuclear Science Division, Lawrence Berkeley Laboratory
Berkeley, CA 94720

1. Abstract

A proposed experiment is described to search for dark-matter axions in the mass range 0.6-16 μeV. The method is based on the Primakoff conversion of axions into monochromatic microwave photons inside a tunable microwave cavity in a large volume high field magnet, as described by Sikivie [1]. This proposal capitalizes on the availability of two Axicell magnets from the decommissioned MFTF-B fusion machine at LLNL. Assuming a local dark-matter density in axions of $\rho = 0.3$ GeV/cm^3, the axion would be found or ruled out at the 97% c.l. in the above mass range in 48 months.

2. Introduction

Generically, the mass of the axion and all its couplings to matter and radiation are proportional to f_A^{-1}. This f_A is the symmetry breaking scale of the Peccei-Quinn symmetry, postulated to provide a mechanism for enforcing CP conservation in the strong interaction. As laboratory experiments and arguments based on stellar evolution constrain the mass of the axion to be less than 10^{-3} eV, it was long thought that such axions, even if abundant from their production in the early universe, would be rendered effectively invisible by the weakness of their couplings. Sikivie [1] showed that this was not necessarily so, and proposed a simple and elegant technique for their conversion and detection as microwave photons in a tunable microwave cavity in a sufficiently strong magnetic field. (A detailed description of this technique is found elsewhere in this volume, as well as results from two pilot experiments [2].) The coherent production of a cold Bose-condensed gas of axions in the early universe has the feature that their contribution to the total mass of the universe goes roughly inversely to the axion mass. From this it is generally argued that closure density would correspond to an axion mass of $m_a < 10$ μeV (subject to an uncertainty estimated to be a factor of 10 either way), which provides a loose lower bound on the axion mass. In inflationary models it is possible that the axion mass could be even smaller than 10^{-6} eV without violating the cosmological bound [3]. Furthermore there is a controversy about whether the overclosure bound on m_a may not be dominated by the mechanism of axion production by radiation from axionic cosmic strings. This is a somewhat technical discussion still under dispute, and only relevant in the case of a non-inflationary scenario or one in which the PQ symmetry breaking would occur after inflation [4]. From an experimental viewpoint one should take the open window to be $10^{-(3-6)}$ eV, and extend the search lower in mass if one can. Two reviews of the status of the axion with brief pedagogical introductions have recently appeared [5,6].

3. Description of the Detector

As mentioned, the proposed experiment is a fairly straightforward scale-up of two pilot efforts (Rochester/BNL/FNAL (RBF) [7], and the University of Florida (UF) [2,8-10]), the discussion of which does not need to be reproduced here. It is clear that the power sensitivity of the pilot experiments, in the mass range which has been measured, falls short of the expected signal by approximately 10^3. The Florida experiment for example had a sensitive volume of 0.008 m^3 and an average field of 7.5 T, and thus $B^2V = 0.45\ T^2m^3$. The principal advantage of the proposed experiment will be the very much larger magnetic volume.

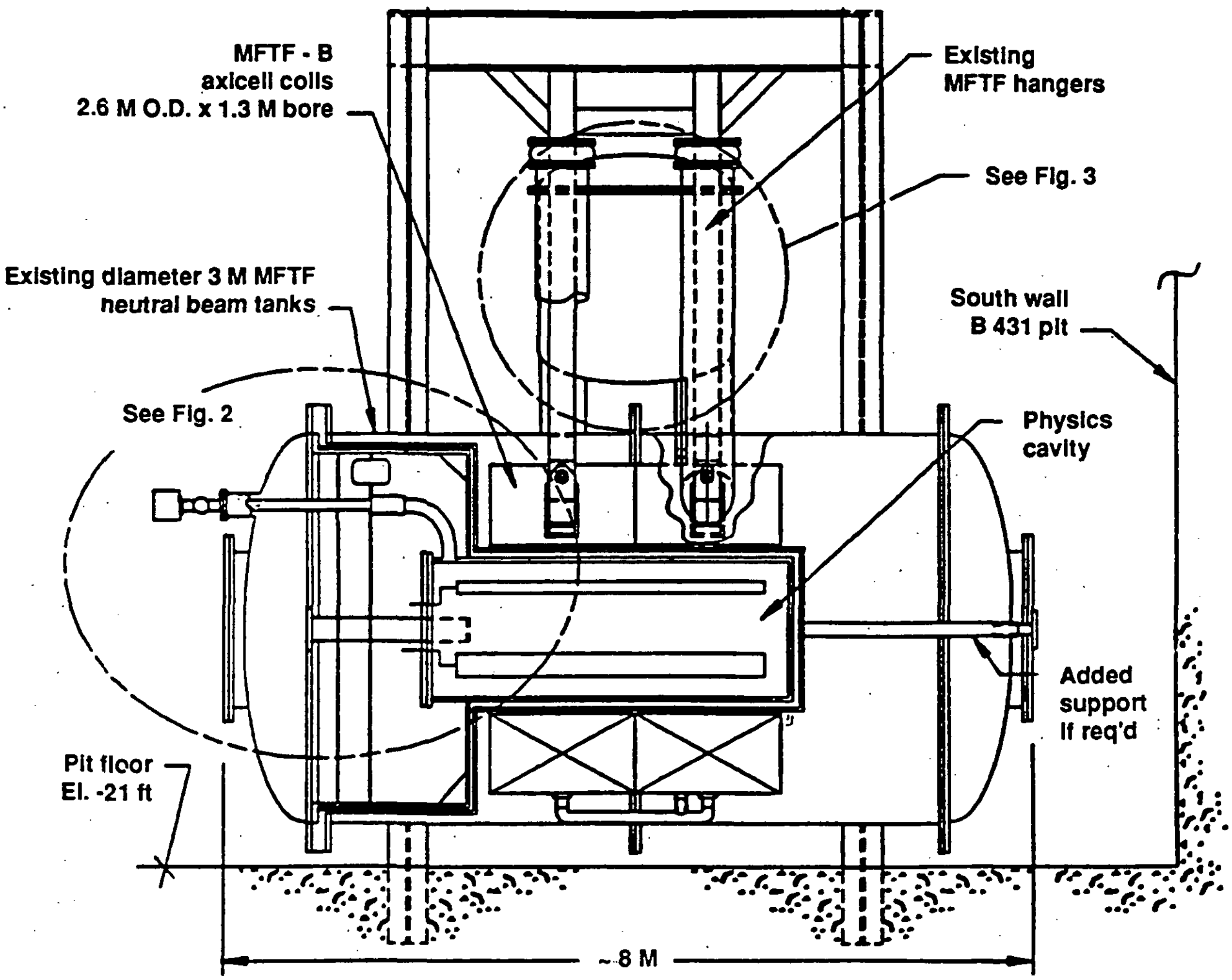

Figure 1. Conceptual design of the axion experiment vessel, showing the magnets, current leads, re-entrant well, microwave cavity, and couplings between the outside world and the cavity. Note the vacuum partition between the magnet and the cavity environments.

3.1. The Axicell magnets

The magnetic volume for this experiment will consist of two Axicell magnets to be removed from the decommissioned MFTF-B at Livermore, and placed flush against one another. The Axicell magnets consist of Nb-Ti conductor, layer-wound on an iron spool-piece, of almost 2000 turns each.

The design operating current is 4238 A, or 8.37×10^6 Amp-turns per magnet. Each Axicell magnet has a clear-bore diameter of 1.34 m and is 1.14 m in depth. The total inductance of the pair is 15 Henries, and the total stored energy is 160 MJ at operating current.

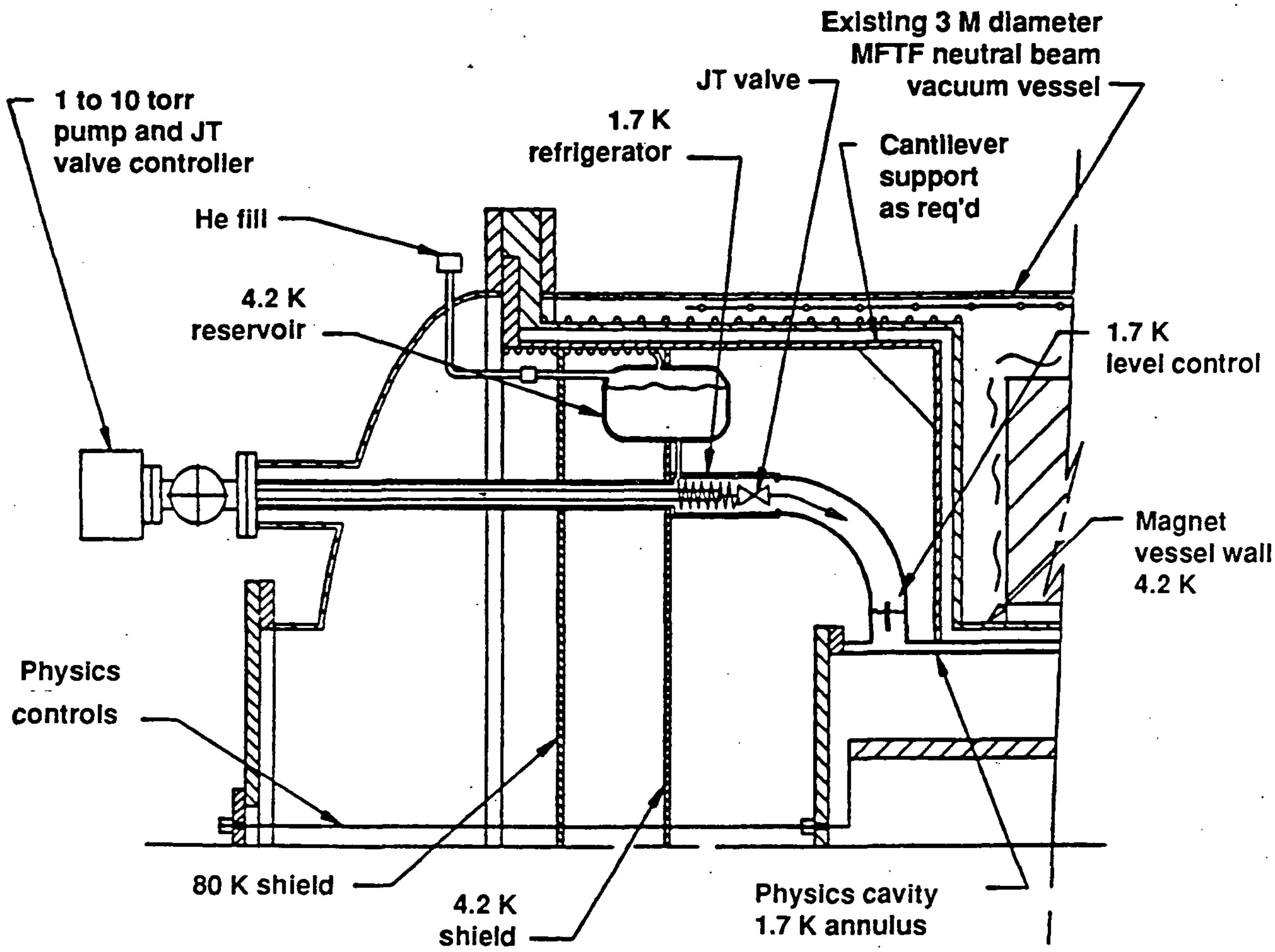

Figure 2. Detail of the refrigerator used for cooling the cavity and cryogenic amplifier.

The magnets will be mounted in a tank (also surplus from the MFTF-B program, a neutral beam injector vessel) with a re-entrant well separating the vacua for the magnets and the copper cavities (Figure 1). This will allow entry and work of short duration on the cavities without breaking vacuum or thermally cycling the magnets. Between the inner radius of the magnet and

the cavity packages is a thin annular 1.7K refrigerator and shield (Figure 2). The coil leads will be modified to work in persistent mode with the switch in the lead stack (Figure 3). The cooling will be performed by a helium refrigerator next to the experiment, utilizing a nearby facility to purify, compress and return the boil-off He. An isometric view of the experiment is shown in Figure 4. The available volume for the microwave cavities is 2.7 m^3, and the r.m.s. value for B_z is 7 T. The major improvement in this experiment over previous experiments is the increase of B_z^2V by approximately 300.

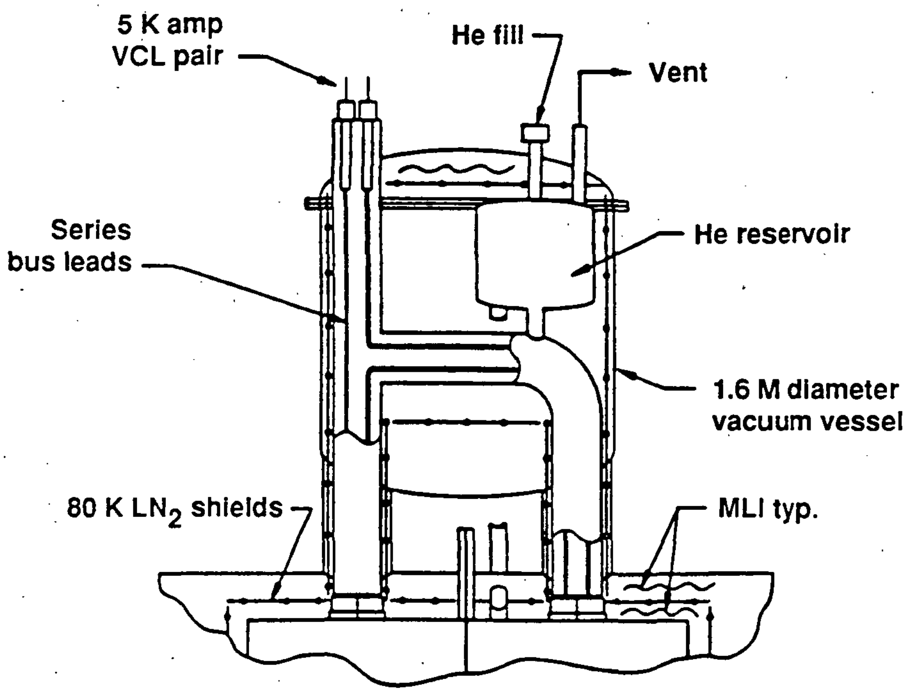

Figure 3. Detail of the current leads and He resevoir tank located above the main tank.

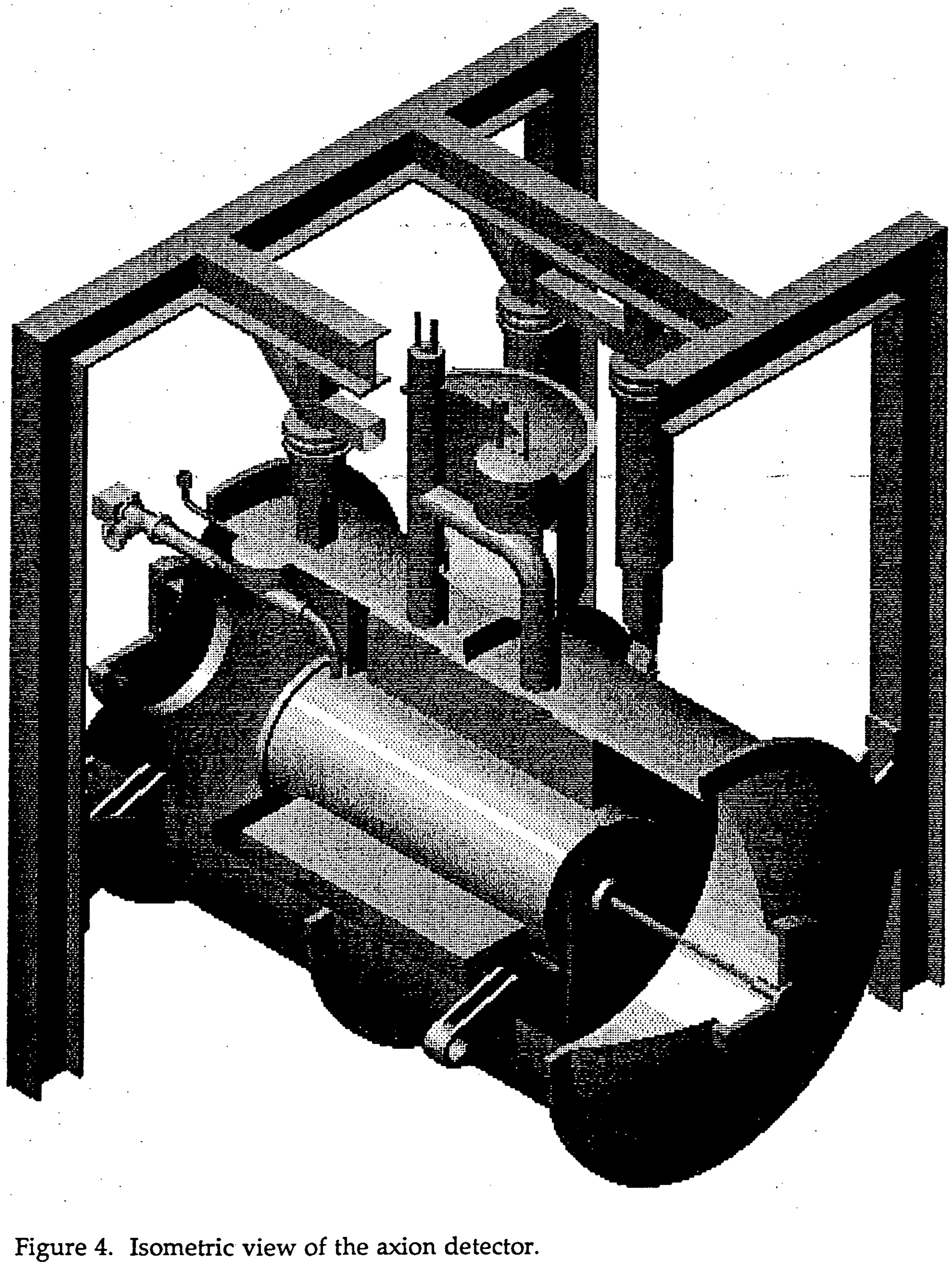

Figure 4. Isometric view of the axion detector.

3.2. The copper cavities

It must be remembered that the diameter of the magnetic volume limits the maximum diameter of a single cavity that may be placed inside, and thus the lowest end of the frequency range that may be searched. The frequency of a right circular cylinder in the TM_{010} mode is given by $\nu = 115/r$, where n is the frequency in MHz, and r is the radius of the cavity in meters. (The TM_{010} mode is the only really feasible one, and thus will be used exclusively in this work.) As $h\nu = mc^2$, the mass range that can be covered is limited by the geometry of the cavities that can be fabricated and inserted into the magnet. (A frequency of 1 GHz corresponds to 4.126 μeV, *etc.*) Cavities may be tuned downward 20% or upward 30% or so by radial displacement of a dielectric rod or metal post respectively without too great a loss in C^2Q [9]. As in the RBF and UF experiments, the cavities must be made of OFHC copper for optimum Q. Furthermore adequate care must be taken in the uniformity of their cross-section to avoid mode localization.

In order to cover a continuous range in masses from 0.6 - 16 μeV (148 - 3900 MHz), nine arrays of cavities are planned. All but the first involve multiple cavities whose outputs are combined through standard power splitter/dividers into a single output. Power splitters/combiners combine the outputs of the cavities without introducing cross-coupling between them. (The nature of the power splitter/dividers available requires that the number of cavities be 2^n.) The first three use essentially the entire available magnetic volume, and are built on a right circular cylinder: (1) undivided; (2) divided into 2 cells of semicircular cross-section; and (3) divided into 4 cells of quarter-circular cross-section. The frequencies of the TM_{010} modes for a semicircular cross-sectional cell, and a quarter-circular cross-sectional cell are $f' = 1.56f$, and $f'' = 2.1f$ respectively, where f is that for the cylinder without partition (see Figure 5). The second set of three are built upon 8 cylinders -- 7 cylinders surrounding 1 in the center, each of radius $r = 0.30R$, where R is the full radius of the available magnetic volume: (4) undivided cylinders; (5) halved; (6) quartered. The third set of three are based on hexagonal-close-packed cells undivided in cross section: (7) $r/R = 0.11$; (8) $r/R = 0.079$; and (9) $r/R = 0.057$. Here however, it becomes necessary to longitudinally segment the cells to minimize problems associated with unfavorable aspect ratios (length/radius) [9]. In addition to making the translational symmetry requirement easier to fulfill (to avoid mode localization), longitudinal segmentation relieves the problem of mode-crowding. It is desirable to minimize the number of crossings of intruder TE modes through the TM_{010} mode. Whenever this happens, mode-mixing occurs and a notch in the tuning range is lost. In order to keep the total lost tuning range to <1%, we choose two-fold segmentation for array (7), and fourfold for (8),(9). With these arrays, and use of dielectric and metal tuning rods, it is possible to cover the proposed mass range continuously (Table I).

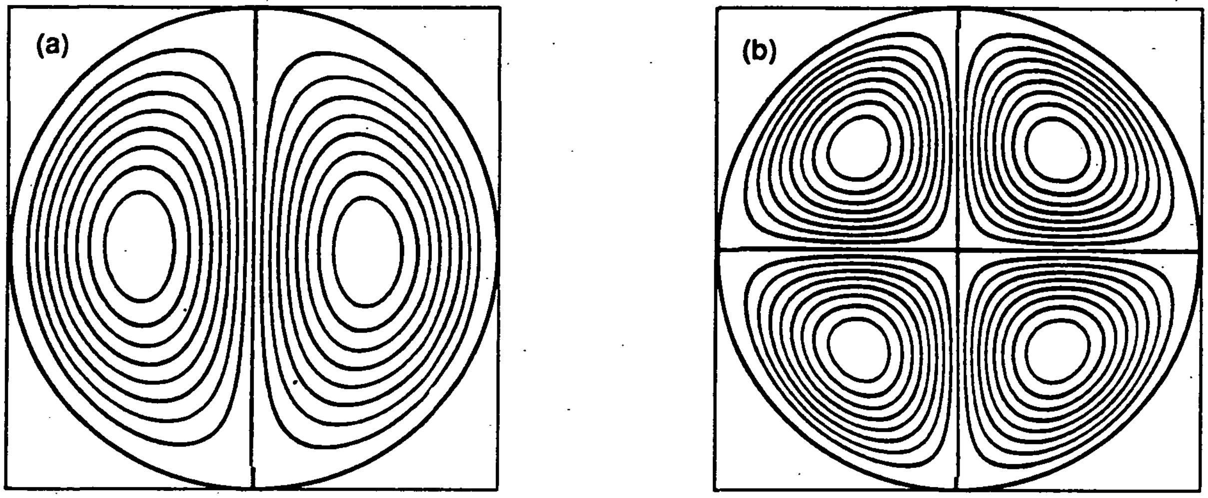

Figure 5. Contours of the TM_{010} mode electric field strength for the cases of (a) semicircular cross-section cavities, and (b) quarter-circular cross-section cavities, made by longitudinal partitioning of a right circular cylindrical cavity.

Power combining of multiple cells involves some care. Prior to each data collection run, one cell (the master) must first be stepped in frequency, and the others (slaves) must be tuned in turn to the frequency of the first. Also it is important that the signal cables of all the cells to the power combiner be of the same length, and the coupling Q_h and the central

Number of cavities	Arrangement	r/R	Packing fraction	Frequency MHz	Tuning Range MHz
1	○	1	1	180	148–233
2	⊖	1	1	281	233–325
4	⊕	1	1	378	325–488
8	○×8	0.30	0.73	595	488–770
16	⊖×8	0.30	0.73	928	770–1070
32	⊕×8	0.30	0.73	1250	1070–1350
128	o×64 × 2	0.11	0.76	1650	1350–1880
512	o×128 × 4	0.079	0.79	2290	1880–2620
1024	o×256 × 4	0.057	0.82	3190	2620–3900

Table I. Parameters of the nine cavity arrays proposed.

frequencies of all the cells be nearly the same, in order to avoid power reflection at the combiner. Combining of two cells at 300K has been demonstrated by Hagmann [10]. We will learn how to handle the practical problems that may arise as one starts from low-order arrays to progressively higher order (and presumably more challenging) arrays, as we proceed.

4. Operation and Proposed Sensitivity

4.1. Search Rate.

The power on resonance from the conversion of axions to photons [2] in the TM_{nl0} mode is given by

$$P_{nl} = \left(\frac{\alpha}{\pi} g_\gamma \frac{1}{f_A}\right)^2 V\, B_z^2\, \rho_a\, C_{nl} \frac{1}{m_a} \mathrm{Min}(Q_L, Q_a) \qquad (1)$$

where C_{nl} is a mode-dependent form factor, Q_L is the loaded quality factor of the cavity and $Q_a \sim 10^6$ is the "quality factor" of the galactic halo axions, *i.e.* the ratio of their energy to their energy spread. This can be rewritten conveniently in terms of benchmark values for all parameters as follows

$$P_{nl} = 3\text{x}10^{-26}\,\mathrm{Watt}\left(\frac{V}{3\ \mathrm{m}^3}\right)\left(\frac{B_z}{7\ \mathrm{Tesla}}\right)^2 C_{nl}\left(\frac{g_\gamma}{0.36}\right)^2 \cdot \left(\frac{\rho_a}{5\text{x}10^{-25}\ \mathrm{g/cm}^3}\right)\left(\frac{m_a}{2\pi(1\mathrm{GHz})}\right)\mathrm{Min}(Q_L, Q_a)\,. \qquad (2)$$

The benchmark value for the axion-photon coupling, 0.36, applies to the simplest axion models, for example that of Dine, Fischler, Srednicki and Zhitnitskii (DFSZ) [11]. In other models, g_γ can be larger or even smaller.

The search rate (df/dt) involves not only the expected conversion power, but also upon the total noise (the sum of the physical temperature of the cavity and the noise temperature of the microwave receiver), the desired signal-to-noise ratio, s/n, and the cavity Q. The search rate is given by

$$\frac{df}{dt} = \frac{55\ \mathrm{GHz}}{\mathrm{year}}\left(\frac{4}{s/n}\right)^2\left(\frac{V}{3\ \mathrm{m}^3}\right)^2\left(\frac{B_z}{7\ \mathrm{Tesla}}\right)^4\left(\frac{g_\gamma}{0.36}\right)^4 \cdot C^2\left(\frac{\rho_a}{5\text{x}10^{-25}\mathrm{g/cm}^3}\right)\left(\frac{5\ \mathrm{K}}{T_n}\right)^2\left(\frac{f}{1\ \mathrm{GHz}}\right)^2\left(\frac{Q_w}{Q_a}\right)\,. \qquad (3)$$

The dependence on Q_w is particular to the case of $Q_w < 3Q_a$, which will always pertain in the present experiment. Here Q_w (w = "wall") is the quality factor that would be achieved if absorption in the walls were the only mechanism for removing energy from the cavity. The other contribution is due to the output coupler, Q_h (h = "hole"), and the loaded Q of the cavity, Q_L is given by $Q_L^{-1} = Q_w^{-1} + Q_h^{-1}$. In the limit where $Q_w < 3Q_a$, the search rate is maximized by the choice of $Q_h = Q_w/2$. The intrinsic cavity quality factors have been calculated for oxygen-free high conductivity copper in the anomalous skin-depth limit.

The cavity bandwidth exceeds the anticipated width of the axion line throughout the search range by characteristically an order of magnitude or more. Thus at each central frequency a fast Fourier transform is performed during the integration time of the run, and a power spectrum collected in bins of width approximating the expected width of the axion line. Each spectrum will be searched for 2σ peaks in single bins and combinations of neighboring bins. If a 2σ peak is found, another set of spectra will be taken and averaged with the first. If the peak remains statistically significant this process will be repeated up to a maximum of 5 times, after which the peak will be flagged for later investigation. The total search rate therefore must take into account the rescan frequency (80% of the spectra are expected to have positive peaks exceeding 2σ and will be repeated at least once), and further the degree to which adjacent spectra are overlapped. A more explicit rendering of eqn. (3) is given below, assuming the DFSZ value of g_γ, a local halo density of 5×10^{-25} g/cm^3 (assumed to be entirely axionic), $Q_a = 10^6$, and a volume of 2.8 m^3 available for the cavities

$$\frac{1}{f}\frac{df}{dt} = \frac{4.9\%}{\text{week}}\left(\frac{4}{s/n}\right)^2\left(\frac{B_z}{7\ \text{Tesla}}\right)^4 P^2C^2\left(\frac{5\ \text{K}}{T_n}\right)^2\left(\frac{f}{1\ \text{GHz}}\right)\left(\frac{Q_w}{10^5}\right)\left(\frac{1}{N_{rescan}}\right)\left(\frac{\Delta f}{\delta f}\right). \qquad (4)$$

In eqn. (4), P is the packing fraction of cavities in the volume, N_{rescan} is the average number of times a given region is rescanned on account of persistent 2σ peaks, Δf is the frequency interval between successive spectra, and $\delta f = f/Q_L$ is the cavity bandwidth. The overlapping of adjacent spectra will be approximately 20%. Table II presents the tuning ranges, expected total noise temperature, quality factors, fractional search rate and total run time for each cavity array. The total time for the experimental program will also include some down time, both for changing of cavity arrays, and also for the tuning of multicavity arrays prior to each run. The scan rate is between 1.3 and 2.1% per week. To achieve a signal-to-noise ratio of 4 for DFSZ axion, the total run time would be under 4 years. If (s/n) were to be raised to 5, the time would be 6 years; if reduced to 3, it would be 2.1 years.

Number of cavities	Arrangement	Tuning Range MHz	T_n K	Q_w	$\frac{1}{f}\frac{df}{dt}$ %/wk	Time weeks
1	○	148–233	6	530000	1.3	36
2	⊖	233–325	6	370000	1.4	23
4	⊕	325–488	6	300000	1.9	24
8	○×8	488–770	5	280000	1.8	27
16	⊖×8	770–1070	5	190000	1.9	17
32	⊕×8	1070–1350	5	160000	2.1	11
128	o×64 × 2	1350–1880	6	150000	2.0	16
512	o×128 × 4	1880–2620	7	130000	1.8	18
1024	o×256 × 4	2620–3900	9	100000	1.7	24

Table II. Search rate of the proposed experiment. Rate and time estimates were made with under the condition that a DFSZ axion would be seen with (s/n) = 4, and presumes the intrinsic cavity quality factors and effective total noise temperatures as shown.

4.2. Summary of proposed experiment

The scope of the proposed experimental search is shown in Figure 6. The ordinate is in $g_{a\gamma\gamma}^2$, where $g_{a\gamma\gamma} = \left(\frac{\alpha}{4\pi} g_\gamma \frac{1}{f_A}\right)$. Shown also are results from the Rochester-Brookhaven-Fermilab, and University of Florida pilot experiments, as well as the DFSZ and KSVZ [12] model predictions between the mass and coupling. We propose to cover the region between 0.6 and 16 μeV, with a s/n = 4. A more complete description of the experiment is found in reference [13].

If the axion is successfully excluded in the region indicated, it would be very interesting to pursue the search upward in mass. As this implies cavities of smaller radii yet, it may be unwieldy to carry this out with a larger number of cavities yet in the same volume. At this point one should consider the use of Axicell insert coils to boost the field to a value of about 14 Tesla, albeit for a diameter of only 30 cm, and a total length of about 100 cm. The overall loss in B^2V of about a factor of 8 would be compensated for in the simplicity of dealing with many fewer cavities.

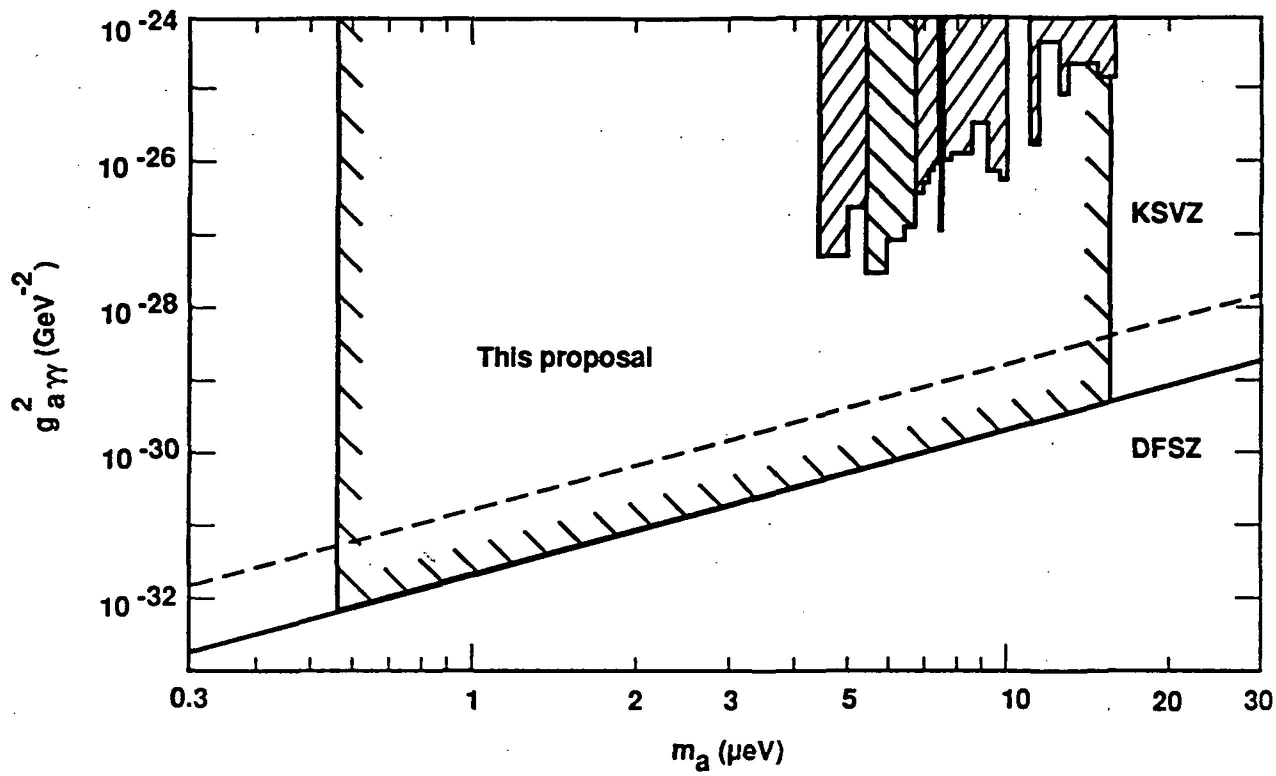

Figure 6. Experimental limits on the electromagnetic coupling $g_{a\gamma\gamma}$ of the axion. Values in the shaded areas at upper right have been excluded by the RBF and UF searches. Values equal to or greater than the DFSZ limit for an axion mass between 0.6 and 16 μeV would be ruled out by this experiment.

We would like to thank John R. Miller, Stewart Shen, Don Slack and Dick Patrick of the Applied Research Engineering Division at LLNL for their design of the magnet and cold-bore facility for this experiment. This work was performed under the auspices of the US Department of Energy at Lawrence Livermore National Laboratory under contract no. W-7405-ENG-48, at the University of Florida under grant no. FG05-86ER-40272, at the University of Chicago under grant no. FG02-90ER-40560, and at Fermilab.

5. References

[1] P. Sikivie, Phys. Rev. Lett. 51 (1983) 1415

[2] C. Hagmann, proceedings of this workshop and references therein (1991)

[3] S.Y. Pi, Phys. Rev. Lett. 52 (1984) 1725; M.S. Turner, Phys. Rev. D33 (1986) 889; A.D. Linde, Phys. Lett. B201 (1988) 437; M.S. Turner and F. Wilczek, Phys. Rev. Lett. 66 (1991) 5

[4] R. Davis, Phys. Lett. 180B (1986) 225; R. Davis and E.P.S. Shellard, Nucl. Phys. B324 (1989) 167; A. Dabholkar and J.M. Quashnock, Nucl. Phys. B333 (1990) 815; D. Harari and P. Sikivie, Phys. Lett 195B (1987) 361; C. Hagmann and P. Sikivie, University of Florida preprint UFIFT-HEP-90-30 (1990)

[5] M.S. Turner, Phys. Rep. 197 (1990) 67

[6] G.G. Raffelt, Phys. Rep. 198 (1990) 1

[7] S. DePanfilis *et al*, Phys. Rev. Lett. 59 (1987) 839; Phys. Rev. D40 (1989) 3153

[8] C. Hagmann *et al*, Phys. Rev. D42 (1990) RC1297

[9] C. Hagmann *et al*, Rev. Sci. Instrum. 61 (1990) 1076

[10] C. Hagmann, PhD thesis, University of Florida (1990)

[11] M. Dine, W. Fischler, M. Srednicki, Phys. Lett. 104B (1981) 199; A.P. Zhitnitskii, Sov. J. Nucl. Phys. 31 (1980) 260

[12] J. Kim, Phys. Rev. Lett. 40 (1977) 223; M.A. Shifman, A.I. Vainshtein, V.I. Zakharov, Nucl. Phys. B166 (1980) 493. In Figure 6, the dashed line is shown for the KSVZ model evaluated with a value of the electromagnetic anomaly of 0, for purely historical reasons. This corresponds to $g_\gamma = 0.97$.

[13] P. Sikivie *et al*, "Experimental Search for Dark-Matter Axions in the 0.6-16 μeV Mass Range", Proposal to the US Department of Energy and the Lawrence Livermore National Laboratory (1990)